Virus Research 323 (2023) 198975

Contents lists available at ScienceDirect

Virus Research

journal homepage: www.elsevier.com/locate/virusres

Evolution of the orthopoxvirus core genome

Cristian Molteni [a,1,*], Diego Forni [a,1], Rachele Cagliani [a], Alessandra Mozzi [a], Mario Clerici [b,c], Manuela Sironi [a]

[a] Scientific Institute IRCCS E. MEDEA, Bioinformatics, Bosisio Parini, Italy
[b] University of Milan, Milan, Italy
[c] Don C. Gnocchi Foundation ONLUS, IRCCS, Milan, Italy

ARTICLE INFO

Keywords:
Orthopoxvirus
Poxviridae
Positive selection
Molecular evolution

ABSTRACT

Orthopoxviruses comprise several relevant pathogens, including the causative agent of smallpox and monkeypox virus. Analysis of orthopoxvirus genome evolution mainly focused on gene gains/losses. We instead analyzed core genes, which are conserved in all orthopoxviruses. We show that, despite their strong constraint, some genes involved in viral morphogenesis and transcription/replication were targets of pervasive positive selection, which was relatively uncommon in immunomodulatory genes. However at least three of the positively selected genes, E3L, A24R, and H3L, might have evolved in response to immune selection. Episodic positive selection was particularly common on the internal branches of the orthopox phylogeny and on the monkeypox virus lineage. The latter showed evidence of episodic positive selection at the D14L gene, which encodes a modulator of complement activation (MOPICE). Notably, two genes (B1R and A33R) targeted by episodic selection on more than one branch are involved in forms of intra-genomic conflict. Finally, we found that, in orthopoxvirus proteomes, intrinsically disordered regions (IDRs) tend to be less constrained and are common targets of positive selection. Extension of our analysis to all poxviruses showed no evidence that the IDR fraction differs with host range. Conversely, we found a strong effect of base composition, which was however not sufficient to explain IDR fraction. We thus suggest that, in poxviruses, the IDR fraction is maintained by modulating GC content to accommodate disorder-promoting codons. Overall, our data provide novel insight in orthopoxvirus evolution and provide a list of genes and sites that are expected to modulate viral phenotypes.

1. Introduction

The *Poxviridae* family includes a number of diverse double-stranded (ds) DNA viruses with large genomes, ranging in length from ~135 to ~350 kbp. Poxviruses infect a wide spectrum of hosts, including insects, birds, reptiles, and mammals (Alonso et al., 2020; Gyuranecz et al., 2013; Lefkowitz et al., 2006; Moss, 2013; Sarker et al., 2019). Thus, the *Poxviridae* family is divided into two subfamilies, *Chordopoxvirinae* and *Entomopoxvirinae*, for viruses that infect vertebrates and invertebrates, respectively. Chordopoxviruses are further classified into 18 genera (https://talk.ictvonline.org/ictv-reports/ictv_9th_report/dsdna-viruses-2011/w/dsdna_viruses/74/poxviridae). Among these, the *Orthopoxvirus* genus comprises several viruses of great medical relevance, including variola virus (VARV), the causative agent of smallpox, and vaccinia virus (VACV), which was used in the smallpox eradication campaign (Fenner et al., 1988). Additional orthopoxviruses with zoonotic potential such as monkeypox virus (MPXV) and cowpox virus (CPXV), are increasingly reported as a cause of human disease, possibly because of waning population immunity caused by discontinuation of routine smallpox vaccination (Beer and Rao, 2019; Silva et al., 2020; Simpson et al., 2020). Indeed, a recent multi-country MPXV outbreak outside of Africa has generated international concerns of possible changes in the epidemiology of this virus (Bunge et al., 2022). In addition to viruses that have been known for decades, recent years have also witnessed the identification of novel orthopoxviruses in humans and other animals. Thus, Akhmeta (AKMV) and Alaska (AKPV) viruses have been sequenced in the last 15 years from people living in Georgia and Alaska (Gao et al., 2018; Gigante et al., 2019), whereas orthopoxvirus Abatino (OPVA) was first isolated in Italy during an outbreak in captive macaques in 2015 (Cardeti et al., 2017). To date, 12 orthopoxvirus species have been officially recognized by the ICTV (https://talk.ictvonline.org/ictv-reports/ictv_9th_report/dsdna-viruses-2011/w/dsdna_vir

* Corresponding author.
E-mail address: cristian.molteni@lanostrafamiglia.it (C. Molteni).
[1] These authors contributed equally to this work.

https://doi.org/10.1016/j.virusres.2022.198975
Received 20 July 2022; Received in revised form 17 October 2022; Accepted 18 October 2022
Available online 21 October 2022

uses/74/poxviridae). Phylogenetically, orthopoxvirus genomes form two major clades of viruses sampled in the Old World and in the New World (Fig. 1). Alaska virus, still not formally classified, forms a distinct clade within the orthopoxvirus diversity (Gigante et al., 2019). Also, CPXV, despite being classified in a single species, is known to be polyphyletic and most likely a composite of different species (Carroll et al., 2011; Franke et al., 2017) (Fig. 1).

Distinct orthopoxviruses largely differ in their host range. For instance, VARV and camelpox virus (CMLV) can only infect humans and camels, respectively, whereas CPXV and MPXV most likely have their natural reservoirs in rodents but can infect a wide range of mammals (Silva et al., 2020). It is commonly held that adaptation of orhopoxviruses to specific hosts is the result of reductive evolution (Hatcher et al., 2014; Hendrickson et al., 2010; Senkevich et al., 2021). This is a situation whereby coding sequences that facilitate infection of multiple hosts are gradually lost by mutation, although instances of adaptive gene loss probably also occurred (Senkevich et al., 2021). However, the wider history of poxvirus genome evolution also witnessed waves of gene gains, with host genomes acting as a source of novel poxvirus genes, and gene capture also occurring during orthopoxvirus evolution (Hatcher et al., 2014; Senkevich et al., 2021; Upton et al., 2003). The net result is that, like all poxviruses, orthopoxviruses have plastic genomes characterized by a central region occupied by core genes and peripheral regions with variable gene content and carrying "accessory" genes that mainly encode proteins involved in host-virus interactions (Senkevich et al., 2021). Indeed, experimental evolution studies with VACV, the prototype orthopoxvirus, have shown that copy number amplification of a gene (K3L) encoding an antagonist of protein kinase R (PKR) confers increased fitness to the virus and facilitates the emergence of adaptive amino acid changes in the same K3 protein (Elde et al., 2012). These observations have generated a keen interest in the analysis of poxvirus genome evolution in terms of gene gains and losses (Hatcher et al., 2014; Hendrickson et al., 2010; Senkevich et al., 2021; Upton et al., 2003). The evolution of the core orthopoxvirus genome has also been investigated (Esteban and Hutchinson, 2011; McLysaght et al., 2003), although less extensively. Nonetheless, some virulence determinants and immunomodulatory functions are accounted for by conserved core genes (Albarnaz et al., 2022; Burles et al., 2014; Jarahian et al., 2011; Liu et al., 2015; Maluquer de Motes et al., 2014; Nuara et al., 2008; Senkevich et al., 2008; Sood et al., 2008; Sood and Moss, 2010; Zhang et al., 2000). Also, compared to variable coding sequences, core genes are more likely to become the targets of novel antipoxvirus preventive and therapeutic strategies. We therefore focused on genes that are conserved across all orthopoxviruses to determine the patterns and trajectories of core genome evolution.

2. Materials and methods

2.1. Sequences, gene alignments, and consensus tree

Gene annotations and genome sequences were retrieved from the National Center for Biotechnology Information database (NCBI, http://www.ncbi.nlm.nih.gov/). Genome sequences and viral species were selected on the basis of the ICTV classification (https://talk.ictvonline.org/ictv-reports/ictv_9th_report/dsdna-viruses-2011/w/dsdna_viruses/74/poxviridae), with the addition of the Alaskapox virus (Gigante et al., 2019). In the case of CPXV, four sequences were included to be representative of major clades (Franke et al., 2017) (Fig. 1, Table 1, Supplementary Table S1). For VACV, the horsepox virus sequence, possibly representing a natural isolate, was selected (Duggan et al., 2020; Tulman et al., 2006). For VARV, an Indian isolate sampled in 1964 was preferred over the reference strain, as the latter has an unknown passage history and was sequenced by subcloning (Shchelkunov et al., 1993). The CPXV reference strain was not included for similar reasons (Archard and Mackett, 1979). In all other cases, reference strains were used.

The whole genome alignment was obtained using Progressive Mauve (v.2.3.1) (Darling et al., 2004, 2010), a tool that aligns genome sequences by taking into account the presence of large deletions, rearrangements, and inversions. Mauve identifies and aligns regions of local collinearity; each block is a region of homologous sequences shared by two or more genomes. Using collinear block information and the Mauve output, we identified one-to-one orthologous genes that were present in all the 16 species analyzed. This generated a dataset of 123 orthologous genes (Supplementary Table S1).

Gene alignments were generated using the GUIDANCE2 suite (Sela et al., 2015), setting sequence type as codons and using MAFFT (Katoh and Standley, 2013) as an aligner. GUIDANCE2 also allows to filter unreliably aligned positions; we removed codons with a score lower than 0.90 (Privman et al., 2012). Finally, the resulting alignments were manually checked.

A consensus tree of the 16 viruses was constructed from a concatenated alignment of 49 conserved genes using IQ-TREE v.1.6.12 (Trifinopoulos et al., 2016). IQ-TREE selects the best-fitting evolutionary model and then generates a maximum-likelihood tree. Branch supports were calculated using the ultrafast bootstrap method (1000 boostraps).

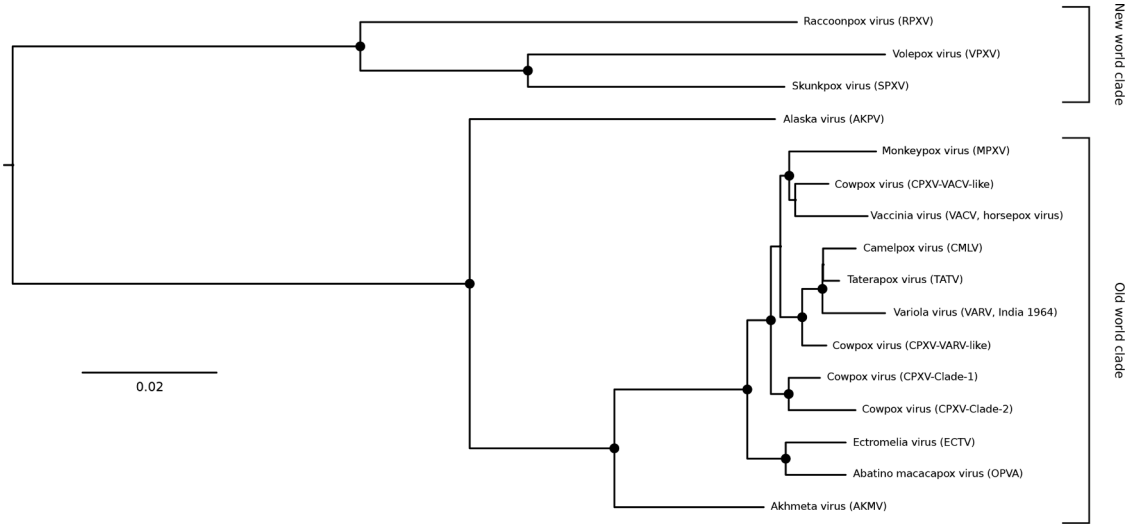

Fig. 1. *Consensus phylogenetic tree of the 16 orthopoxviruses analyzed in this study*. The tree was generated with IQ-TREE v.1.6.12 (Trifinopoulos et al., 2016) using a concatenated alignment of 49 genes conserved in poxviruses. Nodes with bootstrap support higher than 0.8 are labeled with a dot.

Table 1
Virus sequences used in this study.

Accession	Virus	Description/strain	Isolation date	Origin	Passage history
DQ792504	Vaccinia virus	Horsepox virus (MNR-76)	1976	Mongolia	Two passages in sheep kidney cells
DQ437586	Variola virus	Clade P1 (major)	1964	India	Two-three passages in monkey kidney cells
NC_003310	Monkeypox virus	Zaire-96-I-16	1996	Democratic Republic of the Congo	Two passages in monkey kidney cells
HQ420893	Cowpox virus	VACV-like	2000	Finland	Two-three passages in monkey kidney cells
LT896731	Cowpox virus	Clade 1	2015	Germany	Propagation in Vero cells
LN864565	Cowpox virus	VARV-like	2009	Germany	Propagation in Vero cells
LN864566	Cowpox virus	Clade2	2011	Germany	Propagation in Vero cells
NC_008291	Taterapox virus	Dahomey 1968	1968	Benin	Two-three passages in monkey kidney cells
NC_055231	Abatino macacapox virus	Abatino	2015	Italy	Direct sequencing from tissues
NC_055230	Akhmeta virus	2013-88	2013	Georgia	Propagation in BSC40 cells
NC_003391	Camelpox virus	M-96	1996	Kazakhstan	Unknown
NC_004105	Ectromelia virus	Moscow	1947	Russia	Unknown
MN240300	Alaska virus		2015	USA	Propagation in different cell lines
KP143769	Raccoonpox virus	Herman	1964	USA	Unknown
NC_031038	Skunkpox virus	USA1978_WA	1978	USA	Passaged once in chorioallantoic membrane, plaque purified three times in Rat-2 cells, and propagated in BSC-40 cells
NC_031033	Volepox virus	USA1985_CA	1985	USA	Passaged once in chorioallantoic membrane, plaque purified three times in Rat-2 cells, and propagated in BSC-40 cells

2.2. Positive selection analyses

All gene alignments were analyzed for the presence of recombination signals using the RDP5 tool (Martin et al., 2020). This tool allows the implementation of several recombination methods. Specifically, we applied four methods (RDP, GENECONV, MaxChi, and Chimera) (Martin and Rybicki, 2000; Martin et al., 2017; Posada and Crandall, 2001; Sawyer, 1989; Smith, 1992) that showed good power (Bay and Bielawski, 2011; Posada and Crandall, 2001). We considered a recombination event as significant if it was detected by at least 3 of these methods (with a p value < 0.05). We identified 14 gene alignments showing at least one recombination event (Supplementary Table S1). We thus masked the identified region in the recombinant sequence(s).

Gene trees for the positive selection analyses were generated with the phyML program (v.3.1) (Guindon et al., 2009); we applied a General Time Reversible (GTR) model plus gamma-distributed rates and 4 substitution rate categories with a fixed proportion of invariable sites.

The average non-synonymous substitution/synonymous substitution rate (dN/dS) was calculated using the M0 model in the codon-based codeml program implemented in the PAML (Phylogenetic Analysis by Maximum Likelihood) suite (Yang, 2007). M0 assumes that all branches of the phylogeny to have the same dN/dS and infers a single value for that phylogeny.

To detect the action of positive selection, a codeml model (M8, positive selection model) that allows a class of sites to evolve with dN/dS > 1 was compared to a model (M7, neutral model) that does not allow dN/dS > 1. To assess statistical significance, twice the difference of the likelihood (ΔlnL) for the models was compared to a $\chi 2$ distribution (2 degrees of freedom) (Yang, 2007). Genes that were significant after FDR correction for all genes analyzed (p value < 0.05) were also tested by comparing the M8 model with another more conservative neutral model (M8a). In this case, twice the difference of the likelihood for the models was compared to a $\chi 2$ distribution with 1 degree of freedom (p value < 0.05) (Yang, 2007).

Positively selected sites were identified by the Bayes Empirical Bayes (BEB) analysis from M8 (with a posterior probability cutoff of 0.90). BEB analysis calculates the posterior probability that each codon is from the site class of positive selection (Anisimova et al., 2002).

In order to identify specific branches with a proportion of sites evolving with dN/dS > 1, the adaptive Branch-Site Random Effects Likelihood method (aBS-REL) was used. This method applies sequential likelihood ratio tests to identify branches under positive selection without *a priori* knowledge about which lineages are of interest (Smith et al., 2015).

2.3. Protein-protein interaction analysis and epitope prediction

Data regarding viral protein-protein interactions were retrieved from a previous work (Mirzakhanyan and Gershon, 2019). Data regarding host-virus protein interactions were retrieved from the literature (Zhang et al., 2009) and from the Virus MINT database (https://maayanlab.cloud/Harmonizome/resource/Virus±MINT). A comprehensive interaction network was built using Cytoscape v3.9.1 (Shannon et al., 2003).

Linear B-cell epitopes were predicted using the B Cell Epitope Prediction Tools from the IEDB webserver (http://www.iedb.org/), using the amino acid sequence of VACV H3 protein as input and with the default threshold (0.5).

Prediction of discontinuous B-cell epitopes was carried out using the Discotope 2.0 webserver (Kringelum et al., 2012), using the 3D-structure of VACV H3 protein as input (PDB id:5ej0) and with a cutoff = -3.7.

2.4. Analysis of intrinsically disordered regions

The fraction of disordered residues for the core proteomes of the 16 orthopoxviruses were calculated using the IUPred3 (Dosztanyi, 2018; Meszaros et al., 2009, 2018) and the Espritz (Walsh et al., 2012) tools. Predictions were run on individual proteins.

For IUPred3, the short disorder prediction type was selected and we defined as disordered all residues in a protein showing a IUPred3 score > 0.5. Espritz was run using X-ray method as prediction type and best Sw as decision threshold (Walsh et al., 2012).

The IUPred3 tool was also applied to a set of 22 proteomes (both core and accessory) that are representative of different genera in the Poxviridae family (Supplementary Table S3).

For all viruses analyzed herein, gene sequences were also retrieved and G+C content was calculated using the ape R package (Paradis and Schliep, 2019).

2.5. Statistical analyses

Differences in dN/dS or in fraction of disordered residues among gene groups were evaluated using Kruskal-Wallis or Wilcoxon rank sum test, when appropriate. Nemenyi tests with $\chi 2$ distribution to account for ties were used as post-hocs using the PMCMRplus R package (htt

ps://CRAN.R-project.org/package=PMCMRplus).

The binomial test was performed by counting, for the positively selected genes, the number of positively selected disordered residues, the total number of positively selected sites, and the fraction of disorder residues compared to the total length of the residues in the positively selected proteins.

All calculations were performed in the R environment.

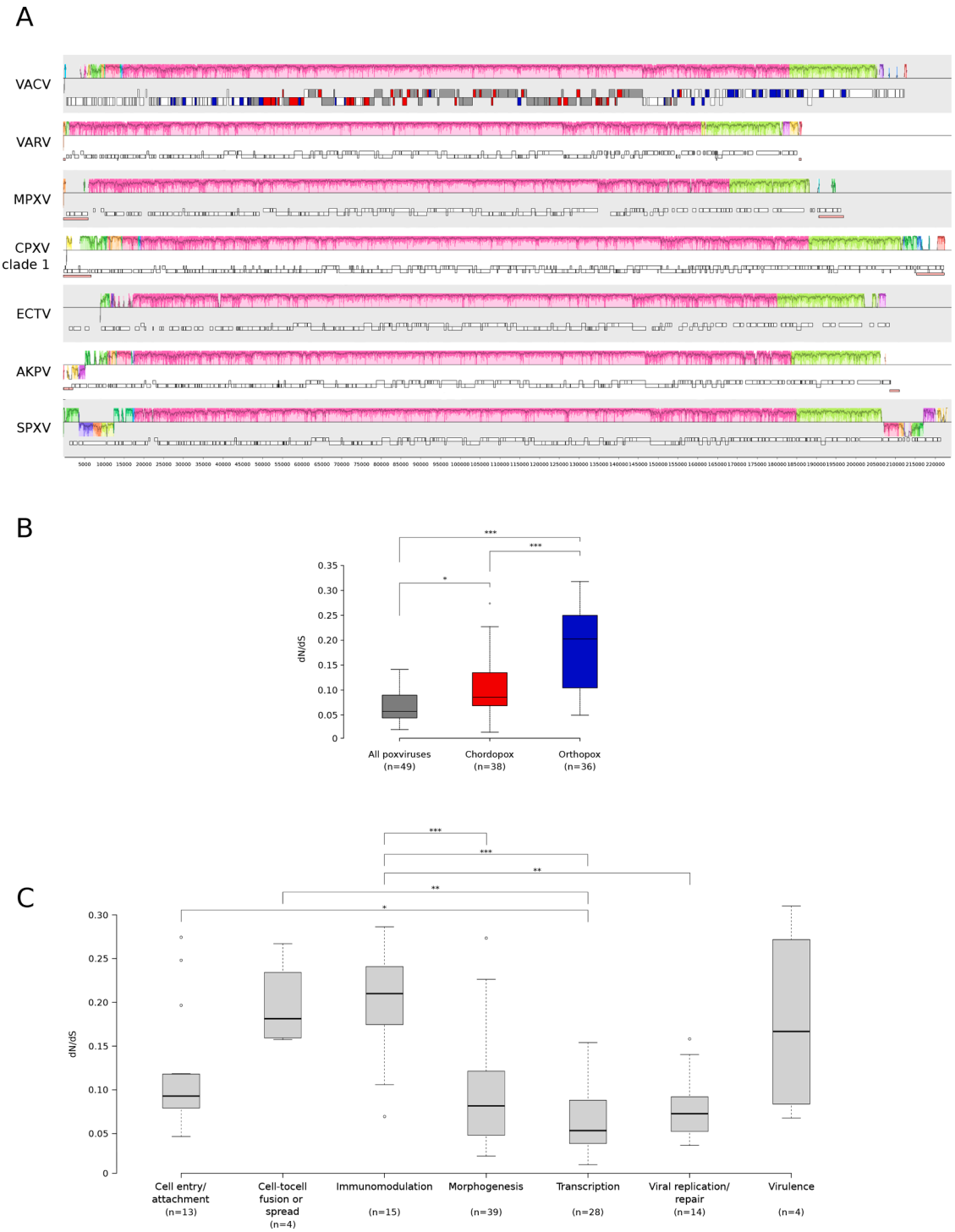

Fig. 2. *Relative evolutionary rates of orthopoxvirus genes.* (A) Whole-genome alignment obtained with progressive Mauve. Each genome is laid out in a horizontal track, with annotated coding regions denoted as boxes. A similarity plot generated by progressive Mauve is shown above each genome, with colors indicating regions that aligns to part of any another genome and thus represent locally collinear blocks. A similarity profile is also plotted within blocks, with height proportional to the level of conservation in that region. For clarity, only few representative viral species are shown. The 123 genes we analyzed in this study are colored in the prototype VACV genome. Colors are according to conservation: grey, genes conserved in all poxviruses; red, genes conserved in chordopoxviruses; blue, genes conserved in orthopoxviruses. (B) Boxplots of dN/dS for the 123 analyzed genes based on their conservation level. Colors are as in panel A. Statistical significance calculated by the Nemenyi post-hoc test is also reported. (C) Boxplots of dN/dS values for the analyzed genes based on their different functional classes. Statistical significance calculated by the Nemenyi post-hoc test is also reported. *, p value < 0.05; **, p value < 0.01; ***, p value < 0.001.

3. Results

3.1. Relative evolutionary rates of orthopoxvirus core genes

With the aim to explore the selective patterns acting on orthopoxvirus genes, we analyzed the genomes of 16 viruses (Table 1, Fig. 1). Eleven of them correspond to recognized species: AKMV, CMLV, Ectromelia virus (ECTV), MPXV, OPVA, Raccoonpox virus (RPXV), Skunkpox virus (SPXV), Taterapox virus (GBLV, also known as TATV), VACV, VARV, and Volepox virus (VPXV). Four additional sequences were selected to represent the major clades within the CPXV genetic diversity (Franke et al., 2017) and one genome represents the recently sequenced AKPV (Gigante et al., 2019) (https://talk.ictvonline.org/ictv-reports/ictv_9th_report/dsdna-viruses-2011/w/dsdna_viruses/74/poxviridae) (Table 1, Fig. 1).

In line with previous observations (Hatcher et al., 2014; Hendrickson et al., 2010; Senkevich et al., 2021; Upton et al., 2003), a whole-genome alignment with Mauve (a method for constructing multiple genome alignments in the presence of large-scale evolutionary events such as rearrangement and deletions/duplications (Darling et al., 2004, 2010)) revealed a large central collinear block, which encompasses the majority of highly conserved genes. Due to gene gains and losses, the terminal genome regions are known to be highly dynamic (Fig. 2A and Supplementary Table S1). In the central region, Mauve identified 123 one-to-one orthologs present in all the genomes. These include 49 genes shared by all poxviruses, 38 conserved in chordopox viruses, and 36 that were common to all orthopox viruses (Fig. 2A) (Upton et al., 2003).

All one-to-one orthologs in the sixteen orthopoxvirus genomes were aligned and rigorously filtered to purge regions or codons with poor alignment quality. After accounting for recombination, we used the codeml M0 model to calculate the average non-synonymous substitution/synonymous substitution rate (dN/dS, also referred to as ω). Comparison among gene groups indicated that dN/dS is significantly different depending on the degree of conservation: genes that are present across all poxviruses have the lowest values, whereas those that are conserved in orthopoxviruses but not necessarily in the other genera or families have the highest (Kruskal-Wallis rank sum test, p value $= 3.55 \times 10^{-11}$) (Fig. 2B).

We next used UniProt and bibliographic sources (Upton et al., 2003) to group viral genes into functional categories (Supplementary Table S1). Comparison of dN/dS among the seven functional classes revealed significant differences (Kruskal-Wallis rank sum test, p value $= 9.02 \times 10^{-08}$). The major contributors to the different evolutionary patterns were genes involved in immunomodulation, cell entry/attachment or cell-to-cell spread. These genes displayed higher dN/dS than those encoding proteins that participate to viral transcription, replication or morphogenesis (Fig. 2C).

3.2. Genome-wide scan for positive selection

The calculation of average dN/dS for viral genes resulted in values below 1, indicating that purifying selection is the major force acting on orthopoxvirus core genomes (Supplementary Table S2). This is consistent with observations on many other viral and non-viral genomes (Lequime et al., 2016; Li et al., 2020; Mozzi et al., 2020a; Sironi et al., 2015; Smith et al., 2013; Wertheim and Kosakovsky Pond, 2011). Nonetheless, positive selection often acts on specific sites in proteins that are otherwise selectively constrained. To test for this possibility, we analyzed the 123 ortholog alignments by applying the "site models" implemented in the codeml tool from the PAML suite (see methods). These models can be used to test whether a gene has experienced positive selection and which sites were the targets thereof. Specifically, we used likelihood ratio tests (LRTs) that compare models of gene evolution that allow (model M8) or disallow (model M7) a class of codons to evolve with dN/dS > 1. After false discovery rate (FDR) correction for multiple tests, 23 genes showed a significant LRT (Supplementary Table S2). These genes were thus tested with a more conservative M8/M8a test. Fifteen of them were significant and were considered targets of positive selection (Table 2, Supplementary Table S2). The specific sites subject to selection were identified using the BEB analysis from M8 (Table 2).

Somehow surprisingly, only two of the positively selected genes are primarily involved in host range control and in immunomodulation. However, one of them (E3L) is a pleiotropic effector with the ability to counteract multiple pathways of the innate immune system (Szczerba et al., 2022). E3L is considered a host range gene in poxviruses and it modulates virulence in mouse models of VACV infection (Brandt et al., 2005; Bratke et al., 2013). The positively selected site we identified (V83) is located in the N-terminal region, which functions as a Z-nucleic-acid-binding domain and is essential for VACV pathogenesis in mice (Szczerba et al., 2022).

Three of the positively selected genes we identified encode proteins with a role in cell-to-cell spread or cell entry/attachment (Table 2). Notably, two such proteins, K2 and A56 interact. The K2/A56 complex prevents cell to cell fusion to avoid syncytia formation (Turner and Moyer, 2008). In turn, this process has a central role in superinfection exclusion, a mechanism that blocks infection of an already infected cell (Turner and Moyer, 2008). The positively selected H3L gene instead encodes a virion envelope protein which binds heparan sulfate on the cell surface. Thus, the protein mediates viral adhesion to the host cell, although it is likely to play a role in virion assembly, as well (da Fonseca et al., 2000; Lin et al., 2000). The protein product is also a major target of neutralizing antibodies (Davies et al., 2005), suggesting that the selective pressure might be exerted by the host humoral immune system. To evaluate this possibility, we predicted linear and conformational B-cell epitopes. Two of the three positively selected sites (P17 and N251) were located in predicted epitopes (Fig. 3).

The majority of positively selected genes is however involved in essential viral functions such as transcription, replication and morphogenesis (Table 2). Nevertheless, mutations in the A24R gene, which encodes the catalytic subunit of the viral RNA polymerase, have been associated with modulation of the RNAse L/PKR pathway, as well as to resistance to the antipoxviral drug isatin-beta-thiosemicarbazone (IBT) (Brennan et al., 2015; Cone et al., 2017; Cresawn et al., 2007). Specifically, mutations (T1121M and D1076G) in the C-terminal portion of A24, where one of the positively selected sites also maps, were associated with PKR evasion and IBT resistance (Brennan et al., 2015; Cresawn et al., 2007). Analysis of the crystal structure of the A24 protein indicated that the other positively selected site (P605) is spatially close to the L18F mutation, which confers fitness trade-offs depending on the cell type or host species (Cone et al., 2017). Three additional genes (E4L, E11L, and A8R) we identified as positive selection targets encode subunits of the RNA polymerase or transcription factors (Table 2). However, no evasion or IBT resistance mutations have to date been reported in the respective proteins. Most of these genes, as well as A20R, encoding a viral DNA polymerase processivity factor, are conserved across chordopoxviruses (Ishii and Moss, 2001). An additional positively selected gene, B1R, encodes a serine-threonine kinase essential for viral DNA synthesis (Lin et al., 1992). The kinase also interacts with a number of cellular proteins, possibly to promote cell survival (Nichols et al., 2006; Santos et al., 2004, 2006).

The remaining positively selected genes are poorly characterized (Table 2). Three of them are involved in different stages of morphogenesis. In particular, the H7 protein contributes to the formation of crescent membranes, a very early event in virion formation (Meng et al., 2013). Conversely, F12 is involved in later stages, as it is necessary for the egress of virions from the host cell (Carpentier et al., 2017), and for actin tail formation (Zhang et al., 2000). Thus, deletion mutants lacking the F12L gene display a small plaque phenotype and are attenuated in a mouse model of infection (Zhang et al., 2000). Finally, E6R is necessary for viroplasm package into viral membranes (Resch et al., 2009).

Table 2
Genes and sites targeted by pervasive positive selection.

Gene name[a]	Functional class	Protein description	Function	Positively selected sites[b]	Fraction of disordered residues (%)	Refs.
A8R	Transcription	32 kDa small subunit of transcription factor VITF-3	Initiates transcription from intermediate gene promoters	Q145 H169 V231	4.04	Sanz and Moss (1999)
A20R	Viral replication/ repair	DNA polymerase processivity factor component A20	Plays an essential role in viral DNA replication	K191 V416	1.88	Ishii and Moss (2001)
A24R	Transcription	DNA-dependent RNA polymerase subunit rpo132	Catalytic subunit of the viral RNA polymerase	P605 V1164*	1.03	Broyles (2003)
A56R	Cell-to-cell fusion or spread	Hemagglutinin	Inhibits cell-cell fusion and reduces superinfection; ineracts with K2	R96	28.14	Turner and Moyer (2008)
B1R	Viral replication/ repair	Serine/threonin kinase	Essential for viral DNA replication; interacts with several cellular proteins	K76 V94 Q296	1.95	Lin et al. (1992), Nichols et al. (2006), Santos et al. (2004, 2006)
C12L	Immunomodulation	Serine protease inhibitor SPI-1	Plays a role in mediating viral host range; may act to inhibit apoptosis	S125	4.61	Liu et al. (2019), Shisler et al. (1999)
E3L	Immunomodulation	Nucleic acid-binding protein	Counteracts multiple pathways of the innate immune system	V83*	11.97	Szczerba et al. (2022)
E4L	Transcription	RNA polymerase subunit	Transcription of early, intermediate, and late genes	A36 A264*	23.88	Broyles (2003)
E6R	Morphogenesis	Hypothetical protein	Late protein which plays an essential role in virion assembly	A194 S428 H564*	1.16	Resch et al. (2009)
E11L	Transcription	Putative virion core protein	Part of the viral RNA polymerase complex	18A	4.90	Grimm et al. (2019)
F12L	Morphogenesis	EEV maturation protein	Virion egress and actin tail formation	Y203 V211 V560 S628	1.25	Carpentier et al. (2017), Zhang et al. (2000)
F8L	Unknown	Hypothetical protein	Protein with iActA-like proline repeats not required for actin tail formation	P20*	61.45	Higley and Way (1997)
H3L	Cell entry/attachment	IMV heparin binding surface protein	Might provide virion attachment to target cell	A63 N251 P17	7.02	Lin et al. (2000)
H7R	Morphogenesis	Hypothetical protein	Formation of crescent membranes	T67	5.96	Meng et al. (2013)
K2L	Cell-to-cell fusion or spread	Serine proteinase inhibitor SPI-3	Inhibits cell-cell fusion and reduces superinfection; ineracts with A56	A3 R183	1.13	Turner and Moyer (2008)

[a] As in VACV Copenhagen nomenclature.
[b] Position refer to the VACV Copenhagen sequence.
*Residue localized into IDRs (intrinsically disordered regions).

3.3. Episodic selection across the orthopox virus phylogeny

The LRTs we applied to search for positively selected genes are devised to detect pervasive positive selection. However, selection is often episodic, acting on a few branches in a phylogenetic tree. Thus, to explore the frequency of episodic positive selection and to assess whether any branch(es) was particularly targeted by it, we applied the adaptive Branch-Site Random Effects Likelihood (aBSREL) model. In particular, we run aBSREL to test whether, on each branch of the phylogeny, a proportion of sites have evolved under positive selection (note that aBSREL does not test for selection at specific sites). This method allowed the identification of 22 genes with at least one branch showing evidence of episodic positive selection (Fig. 4A). Again, these genes belonged to different functional classes, but those involved in morphogenesis were the most abundant (Table 3). Analysis of selection signals indicated that the longer internal branches of the orthopoxvirus phylogeny were frequent targets of selection. Among terminal branches, the lineage showing the strongest evidence of episodic positive selection was MPXV (Fig. 4A and Table 3). Among the four positively selected genes on this branch, one is the ortholog of VACV A33R, which showed evidence of selection on multiple branches (see below). The other three are orthologs of J1R, J6R, and C3L. Whereas J1R and J6R play roles in morphogenesis and transcription, VACV C3L and its MPXV ortholog, D14L (also referred to as MOPICE), function as modulators of the complement system and represent virulence factors (Chen et al., 2005).

Interestingly, two of the four genes showing evidence of episodic positive selection on multiple branches (Fig. 4B), B1R and A33R, are involved in peculiar poxviral mechanisms that control viral fitness and spread. Thus, B1R encodes a protein kinase that antagonizes both a cellular antiviral factor (BAF) and the poxvirus-encoded pseudokinase B12, this latter functioning as a repressor of viral replication (Olson et al., 2019). A33R is instead necessary for superinfection exclusion (Doceul et al., 2010). Specifically, A33 is expressed at the plasma membrane of VACV infected cells and, in concert with other viral proteins, induces the repulsion of superinfecting virions toward uninfected cells. The ultimate effect is not only superinfection exclusion, but also an increase in viral spatial spread (Doceul et al., 2010).

To gain insight into the interaction among genes that were targets of pervasive or episodic positive selection, we retrieved data on both host–virus protein-protein interactions (H-V PPIs) and virus-virus PPIs (V-V PPIs) for the 123 analyzed core genes. We next generated an interaction network. This showed that several positively selected proteins participate to interactions among themselves and with other viral proteins (Fig. 5). Some of the selected proteins (e.g., A24R, H3L, A3L,

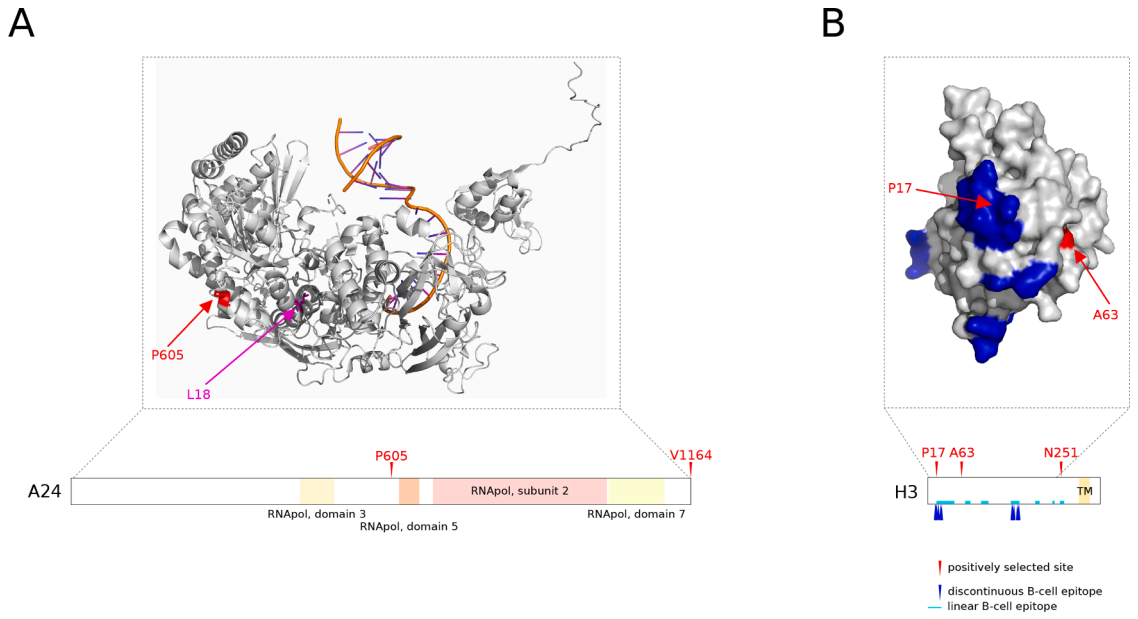

Fig. 3. *Distribution of positively selected sites.* The location of the positively selected sites (colored in red) in the A24 (A) and H3 (B) proteins is shown, both on their schematic protein representation and on the 3D structures. For A24, the position of the functional L18F mutation (see text) is shown in magenta (Cone et al., 2017). For the H3 protein, the location of predicted epitopes is also reported. 3D protein structures were retrieved from the Protein Data Bank (PDB IDs: 6rie and 5ej0).

A10L) represent major hubs in this network, whereas only B13 and E3L show abundant interactions with host proteins.

3.4. Protein evolution and intrinsically disordered regions

In viral and non-viral proteomes, protein regions that are intrinsically disordered (intrinsically disordered regions, IDRs)—that is, domains that do not adopt compact three-dimensional structures— are known to be fast evolving (Afanasyeva et al., 2018; Brown et al., 2010; Dyson and Wright, 2005; Hagai et al., 2014; Mozzi et al., 2020b; Nilsson et al., 2011). Previous studies also indicated that, compared with cellular organisms, viral proteomes have a wider variation in IDR fraction, with poxviruses showing a low representation of IDRs (Kumar et al., 2021; Peng et al., 2015; Pushker et al., 2013; Xue et al., 2014). We thus set out to investigate the relationship between protein relative evolutionary rates and IDR fraction in orthopox viruses. For core proteomes (i.e., the 123 genes shared by all orthopoxviruses), IDRs were predicted using the Espritz X-ray and the IUPRED3 methods (for short disorder). As previously reported (Kumar et al., 2021), the two methods provided very similar estimates (Pearson's product-moment correlation, $r = 0.91$, p value $< 2.2 \times 10^{-16}$). Thus, IUPRED3 was used for subsequent analyses. In agreement with the strong conservation of poxvirus proteins, no significant difference was observed in the fraction of IDRs across the 16 orthopox virus core proteomes (Supplementary Fig. 1). We thus used values averaged over the 16 core proteomes to define disordered residues (average score > 0.5).

Of the positively selected sites we detected, only five out of 30 were located in IDRs. Because of the low abundance of disordered regions in orthopox viruses, this number was nonetheless higher than expected (Binomial test, p value $= 0.038$). In line with this finding, gene-wise analysis of dN/dS and IDR fraction revealed a positive and significant, albeit weak, correlation (Kendall's rank correlation, tau $= 0.14$, p value $= 0.017$). Minor differences in IDR fraction were also detected based on gene conservation (Kruskal-Wallis rank sum test, p value $= 0.026$) (Supplementary Fig. 2A), whereas no differences were observed among functional classes (Supplementary Fig. 2B).

IDRs are frequently involved in PPIs, and data on other dsDNA viruses showed that viral proteins that interact with host factors have a higher fraction of disordered regions (Mozzi et al., 2020b). We thus assessed whether the same tendency is observed for orthopoxvirus proteins. Comparisons indicated that orthopox virus proteins that engage in V-H PPIs have a similar fraction of disordered regions as those that do not (Supplementary Fig. 2C). Also, no differences in IDR fraction was evident for V-V PPIs (Supplementary Fig. 2D).

Finally, we investigated whether differences exist in terms of IDR representation across poxvirus genera. We thus retrieved whole proteome information for 22 viruses that are representative of different genera in the *Poxviridae* family (for orthopoxviruses we used the VACV proteome) (Supplementary Table S3). Calculation of the fraction of IDRs revealed significant differences (Kruskall-Wallis p value $< 2.2 \times 10^{-16}$) with the highest levels observed in molluscipoxviruses and parapoxviruses, the lowest in alpha-, beta-, and deltaentomopoxviruses (Fig. 6A).

Because previous studies showed that the level of protein disorder in viral proteomes is influenced by genome size and base composition (G+C content) (Pushker et al., 2013), we finally correlated the G+C content and length of poxvirus genomes to the average IDR fraction in whole proteomes. Whereas no correlation was observed with genome size, a very strong and positive correlation was detected with G+C content (Spearman's rank correlation rho $= 0.94$, p value $= 4.11 \times 10^{-06}$) (Fig. 6B). This strong relationship may suggest that IDR fraction in poxviruses is simply a secondary effect of genome base composition. To assess this hypothesis we compared the G+C content in IDRs and in the structured regions of the same poxvirus proteins where IDRs are located. Results indicated that, among low-G+C content genomes IDRs tend to have a higher G+C than structured regions, whereas the opposite situation was observed in some high-G+C content genomes (Fig. 6C). Thus, the fraction of IDRs in poxvirus proteomes is not merely the result of base composition, but most likely represents an actively maintained feature.

4. Discussion

Gene-wise estimates of dN/dS indicated that purifying selection is a major force acting on orthopoxvirus genomes and that the strength of selective constraint is stronger for genes involved in core processes such as viral morphogenesis, transcription, and DNA replication or repair. Despite their stronger constraint, though, some of these genes were also

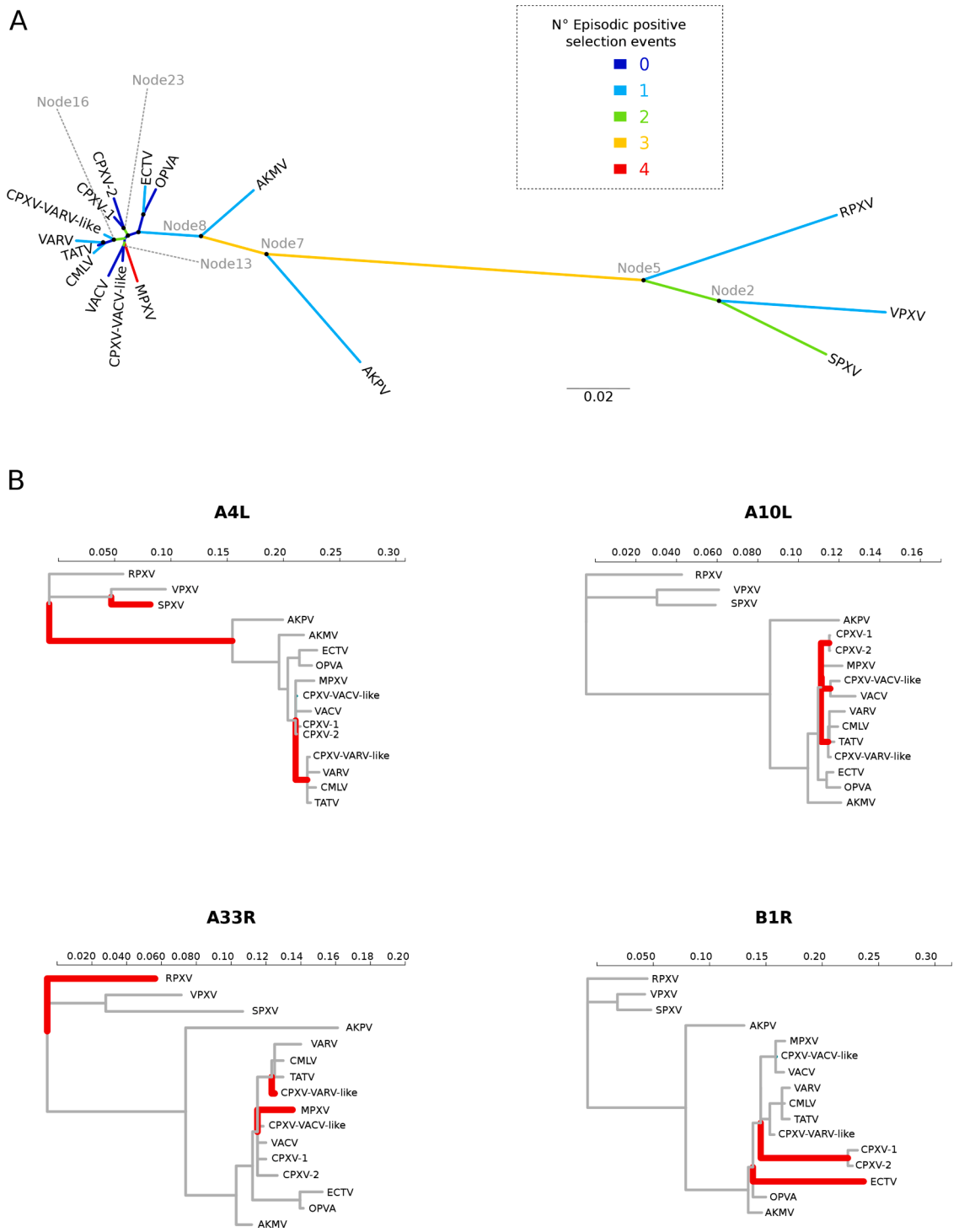

Fig. 4. *Episodic positive selection in orthopoxviruses*. (A) Consensus phylogenetic tree of the 49 genes conserved in all poxviruses. As in Fig. 1, nodes with bootstrap support higher than 0.8 are labeled with a dot. Colors indicate, for all branches, the number of genes that showed evidence of episodic positive selection using aBSREL analysis (see the legend for details). (B) Phylogenetic trees of the four genes for which multiple branches (colored in red) have been found under episodic positive selection.

targets of pervasive positive selection and most of these were conserved in Orthopoxviruses have greatly impacted the course of human history. Smallpox represented one of the most devastating afflictions of human societies, but also became the first (and so far the only) disease to be eradicated through a worldwide vaccination campaign. The vaccinating agent was another orthopoxvirus, VACV. In the modern world, orthopoxviruses still account for a substantial health burden and fears of accidental or deliberate VARV release prompt ongoing research on the virus. Moreover, orthopoxviruses are actively investigated to develop recombinant vaccines and as oncolytic viruses, in addition to representing common laboratory models to study virus evolution and host-pathogen interactions. However, analysis of the evolution of orthopoxvirus genomes has mainly focused on gene gains/losses (Hatcher et al., 2014; Hendrickson et al., 2010; Senkevich et al., 2021; Upton et al., 2003). Here, we focused on core genes - i.e., those that are conserved in 16 recognized or tentative orthopoxvirus species - and we

Table 3
Genes under episodic positive selection.

Gene name[a]	Functional classes	N° of branches under selection	Branch under Episodic selection	aBSREL corrected *p* value
A3L	morphogenesis	1	Node 2	0.01393
A4L	morphogenesis	3	Node 5	0.00164
			Node 16	0.01861
			SPXV	0.00951
A10L	morphogenesis	3	Node 13	<0.00001
			Node 16	0.00133
			Node 23	0.01930
A12L	morphogenesis	1	Node 5	0.00177
A28L	cell entry/attachment	1	Node 7	0.04439
A33R	Cell-to-cell fusion or spread	3	RPXV	0.00478
			CPXV VARV-like	0.02348
			MPXV	0.03736
A56R	Cell-to-cell fusion or spread	1	CMLV	<0.00001
B1R	viral replication/repair	2	Node 23	0.00137
			ECTV	0.01261
B5R	cell entry/attachment	1	Node 13	0.01671
B13R	Immunomodulation	1	Node 8	0.03805
C3L	Immunomodulation	1	MPXV	0.00012
D3R	morphogenesis	1	AKMV	0.01797
D10R	transcription	1	VPXV	0.02118
E3L	Immunomodulation	1	Node 5	0.00279
E10R	morphogenesis	1	AKPV	0.03753
F11L	Cell-to-cell fusion or spread	1	Node 2	0.00396
F12L	morphogenesis	1	Node 7	0.02147
F15L	morphogenesis	1	VARV	0.00011
F17R	morphogenesis	1	SPXV	0.03468
J1R	morphogenesis	1	MPXV	0.03081
J2R	viral replication/repair	1	Node 7	0.04335
J6R	transcription	1	MPXV	0.00100

[a] As in VACV Copenhagen nomenclature.

measured selection using dN/dS, one of the most commonly used metrics. Importantly, the interpretation of dN/dS and its maximum likelihood estimate are based on the assumption that the sequences being compared are sampled from separate populations (Kryazhimskiy and Plotkin, 2008). This is because synonymous and non-synonymous differences among distantly related sequences represent substitutions that have gone to fixation, whereas differences among sequences sampled from a single population represent segregating polymorphisms (Kryazhimskiy and Plotkin, 2008). Thus, although a number of complete genomic sequences are available for different orthopoxviruses, we only analyzed 16 genomes that represent divergent species.or in the whole *Poxviridae* family. This situation is reminiscent of the positive selection patterns observed in cytomegaloviruses, whereby core genes, despite being more constrained, also showed signatures of positive selection (Mozzi et al., 2020a). That finding was interpreted in terms of concerted evolution of genes that concur to the same process, an explanation that might also hold for orthopoxviruses, as some positively selected genes interact physically or functionally, as demonstrated by their PPIs. It should however be added that at least three of the positively selected genes, A24R, E3L, and H3L, might have evolved in response to selective pressures exerted by the host immune system. As mentioned above, mutations in the A24 protein have been associated with evasion of the PKR system, although the underlying mechanisms are unknown. Brennan and coworkers proposed that mutations that emerged in A24R during *in vitro* replication might represent an adaptation to evade dsRNA sensors; the identification of A24R as a target of positive selection suggests that such variants confer a fitness advantage not only during experimental evolution in cell culture but also in natural settings. Notably, E3L also functions as an antagonist of PKR, as well as of other innate immune pathways. The positively selected site is located in the N-terminal domain, which contributes to PKR antagonism, but also binds Z-nucleic acids. Major functions of the E3L N-terminus include the inhibition of necroptosis, a caspase-independent form of programmed cell death, and the counteracting the type I IFN system (Szczerba et al., 2022).

With respect to H3L, the gene encodes an immunodominant protein and a major target of neutralizing antibodies. Indeed, antibodies raised against the VACV H3 protein contribute to cross-protection against other orthopoxviruses (Gilchuk et al., 2016). Two of the positively selected sites were located in predicted B-cell epitopes, suggesting that they evolved to elude humoral immune responses in orthopoxvirus hosts.

The relatively low abundance of pervasive positive selection signals and the fact that these mainly involve genes that are not directly involved in immune modulation, is most likely the consequence of different effects. First, the limited number of sequences affords low power to detect positive selection and the power of the dN/dS statistic is further reduced when the majority of sites in the protein evolve under purifying selection (Kryazhimskiy and Plotkin, 2008). Second, ample evidence indicates that variation in gene copy number in the peripheral regions of poxvirus genomes provides an efficient and versatile mechanism to adapt to selective pressures exerted by the host immune response. Thus, the core genome might experience relatively limited immune-mediated pressures, which instead impinge on accessory genes.

Compared to pervasive positive selection, we found more genes to be targeted by episodic positive selection. The long internal branches of the orthopox phylogeny were preferential targets of episodic selection, as was the MPXV lineage. In analogy to CPXV, MPXV is a zoonotic virus with a broad host range. It is very difficult to speculate on the reason(s) why it experienced selection more frequently than other orthopoxviruses. It is however worth noting that the genetic diversity of MPXV in the endemic region is structured into two major clades: one is mainly transmitted in the Congo Basin (clade1), whereas the other, which is composed of two subclades (clades 2a and 2b), is mainly found in West Africa. A higher virulence of clade 1 viruses compared to those in clade 2 was consistently reported (Bunge et al., 2022). One of the genes showing evidence of episodic positive selection (D14L or MOPICE) functions as a modulator of complement activation and it is only encoded by clade 1 viruses (among which the reference genome is classified), as it is deleted in clade 2 genomes (Chen et al., 2005). Experiments with recombinant MPXV revealed that MOPICE is a virulence factor in clade 1 viruses, at

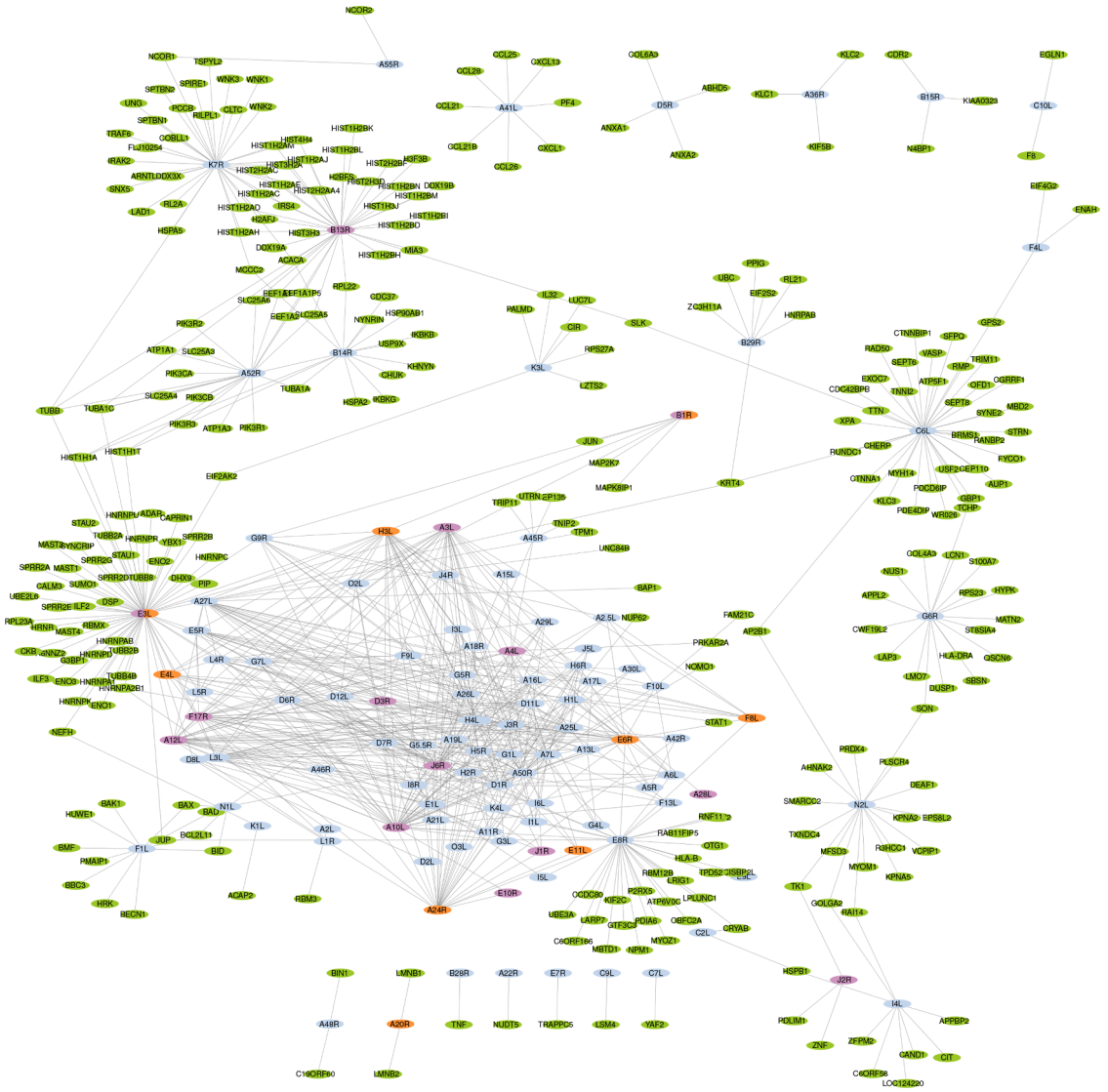

Fig. 5. *Network of protein-protein interactions*. Virus-virus and virus-host protein-protein interactions are shown in a network generated with Cytoscape. Human proteins are shown in green and viral proteins in cyan. Viral proteins under pervasive or episodic positive selection are denoted in orange and violet, respectively. Protein-protein interactions have been retrieved from previous works (see methods for details). Proteins identified as positive selection targets are shown only if at least an interactor is known (therefore they are not all present in the figure).

least in prairie dogs, although it is not the only determinant of the lower pathogenicity of clade 2 MPXV (Hudson et al., 2012). Because the mammalian complement system is also fast evolving, due to host-pathogen conflicts (Cagliani et al., 2016), MOPICE might have evolved to adapt to complement components encoded by MPXV natural reservoir(s). Loss of MOPICE in clade 2/3 viruses might be framed within the common phenomenon of orthopoxvirus reductive evolution or adaptive gene loss.

Another intriguing observation about the signals we detected with aBSREL is that two genes showing evidence of selection on more than one branch are involved in some form of intra-genomic conflict. Thus, the B1 kinase antagonizes another poxvirus-encoded protein (B12), which in turn functions as a repressor of viral replication. The A33 protein is instead involved in superinfection exclusion, a phenomenon that allows faster viral spread, but also excludes from the infected cell additional viral genomes, eventually reducing the opportunities for cheating (Leeks et al., 2021). Notably, two genes (K2L and A56R) involved in a distinct mechanism of superinfection exclusion were also found to be targeted by pervasive positive selection, supporting the view that incoming viruses, even belonging to the same species, act as an important selective pressure. Intra-genomic conflicts have been described in a number of organisms (Gardner and Úbeda, 2017). It will be interesting to assess whether they also play a role in the evolution of viral genes, at least in viruses with complex genomes as orthopoxviruses.

In recent years, evidence has accumulated that IDRs represent a dynamic fraction of viral and non-viral proteomes. IDRs tend to be less constrained and are common targets of positive selection (Afanasyeva et al., 2018; Brown et al., 2010; Dyson and Wright, 2005; Hagai et al., 2014; Mozzi et al., 2020b; Nilsson et al., 2011). Our data confirm a recent analysis of viral proteomes by showing that poxviruses display, on average, a low fraction of IDRs (Kumar et al., 2021). In their study, Kumar and co-workers showed that dsDNA viruses that replicated in the cytoplasm (as is the case of poxviruses) have lower IDR fractions than those that replicated in the nucleus. The authors also showed that, in animal viruses, the IDR fraction tends to negatively correlate with proteome size. These observations might partially explain the low IDR representation in poxviruses. It is also worth noting that, in contrast to herpesviruses, with large dsDNA genomes and a higher fraction of IDRs, poxviruses typically cause acute and transient infections. Whether these differences account for different IDR content remains to be clarified

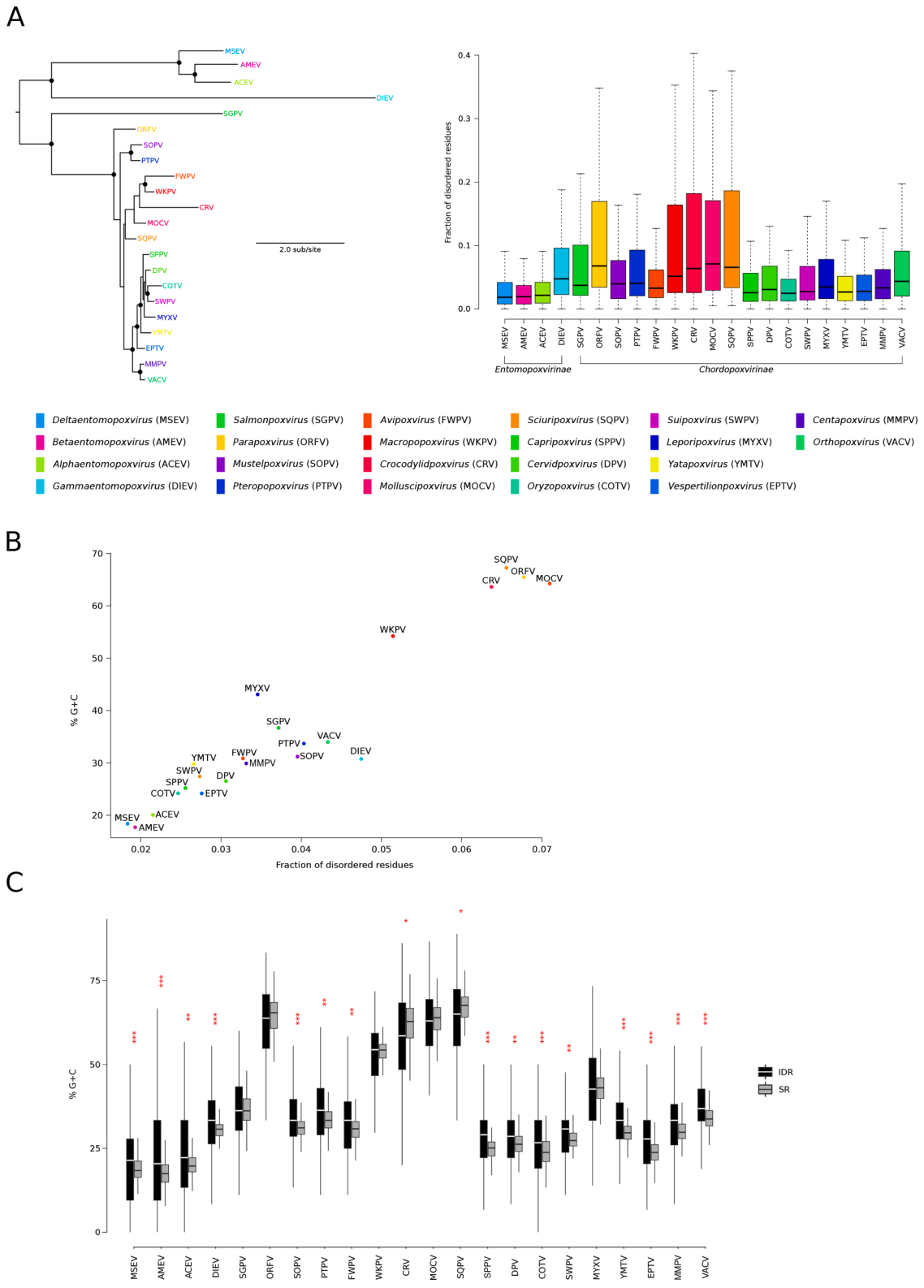

Fig. 6. *Level of protein disorder in poxvirus genera.* (A) Phylogenetic tree of representative members of 22 genera in the *Poxviridae* family. The tree was constructed with IQ-TREE v.1.6.12 (Trifinopoulos et al., 2016) using a protein alignment of VACV H4 (RNA polymerase-associated transcription-specificity factor) orthologs. Nodes with bootstrap support higher than 0.8 are labeled with a dot. The fraction of disordered residues (IUPred3 score > 0.5) was calculated for each protein of the representative viral species in 22 poxvirus genera and plotted as boxplots (see Supplementary Table S3 for virus abbreviation). Viral genera are colored accordingly to the legend. Whole proteomes were analyzed. (B) Correlation plot between the mean fraction of disordered residues per gene and the mean G+C percentage for the 22 representative viral species. Colors are as in panel A. (C) Percentage of G+C content in disordered (IDR) and structured (SR) residues. The G+C content (%) in genes having both disordered and structured residues was calculated and displayed as boxplots. Red asterisks denote a statistical difference (*, p value < 0.05; **, p value < 0.01; ***, p value < 0.001) among IDR and SR for each viral proteome. Statistical significance was calculated using Wilcoxon rank sum tests and corrected for multiple testing using the false discover rate (FDR).

(Kumar et al., 2021). In any case, our data suggest that, as in other viral and non-viral proteomes, IDRs show dynamic evolution in poxviruses. It should however be mentioned that, although we found that positively selected signals are more frequently detected in IDRs than expected by chance, this result is based on a small number of sites. Likewise, the gene-wise correlation between dN/dS and IDR fraction revealed a significant but weak correlation. Additional analyses, possibly over deeper evolutionary distances, might contribute to shed light into the relationship between evolutionary rates and disorder in poxviruses. Also, in contrast to observations in some herpesviruses, orthopoxvirus proteins that interact with host components are not more disordered than those without known host interactors.

It was previously suggested that disordered regions in viral proteins afford evolutionary plasticity and host adaptation while preserving protein function (Hagai et al., 2014; Mozzi et al., 2020b). In fact, in herpesviruses, a higher fraction of IDRs seems to be associated with a wider host range (Mozzi et al., 2020b). We did not find differences among orthopoxviruses in IDR fraction, despite a large diversity in host spectrum. Likewise, no effect of host range was evident when we analyzed representatives of all poxvirus genera. For instance, the highest fraction of IDRs was detected in molluscipoxviruses, which are very well known to infect only humans (McFadden, 2005). These observations, together with the finding that orthopoxvirus proteins that interact with host molecules are not significantly more disordered than those that do not, suggest that IDRs do not play a relevant role in host adaptation in poxviruses. Conversely, we found a very strong effect of base composition on IDR fraction. This is partially expected because residues enriched in disordered regions are mainly encoded by G+C rich codons (Basile et al., 2019; Pushker et al., 2013). Clearly, this observation opens the question as to whether the fraction of IDRs is simply a consequence of base composition or if it is an adaptive feature driven by specific viral characteristics. To indirectly address this question, we thus compared, in the proteins showing evidence of intrinsic disorder, the G+C content of IDRs and of structured regions. Differences were observed in both G+C-poor and in G+C-rich genomes. Although not conclusive, these data suggest that, in poxviruses, the IDR fraction is actively maintained by increasing or decreasing the G+C content to accommodate disorder-promoting codons. Clearly, though, these data have important limitations. The most relevant one is that IDRs were derived from predictions. Although we used two methods and detected very good correspondence, we cannot exclude that biases were introduced and some predictions are inaccurate.

Overall, our data shed light into the evolution of orthopoxvirus genomes and into the distribution and significance of IDRs in the *Poxviridae* family. Because they are expected to modulate viral phenotypes, the positively selected genes and sites we identified should be prioritized in functional analyses.

CRediT authorship contribution statement

Cristian Molteni: Conceptualization, Formal analysis, Investigation, Visualization, Writing – original draft. **Diego Forni:** Conceptualization, Formal analysis, Investigation, Visualization, Writing – original draft. **Rachele Cagliani:** Formal analysis, Writing – review & editing. **Alessandra Mozzi:** Formal analysis, Visualization. **Mario Clerici:** Supervision, Writing – review & editing. **Manuela Sironi:** Conceptualization, Investigation, Supervision, Writing – original draft, Writing – review & editing.

Declaration of Competing Interest

The authors declare that they have no competing interests.

Data Availability

NCBI accession IDs are provided in Supplementary Tables 1 and 3.

Acknowledgment

This work was supported by the Italian Ministry of Health ("Ricerca Corrente 2022" to MS).

Supplementary materials

Supplementary material associated with this article can be found, in the online version, at doi:10.1016/j.virusres.2022.198975.

References

Afanasyeva, A., Bockwoldt, M., Cooney, C.R., Heiland, I., Gossmann, T.I., 2018. Human long intrinsically disordered protein regions are frequent targets of positive selection. Genome Res. 28, 975–982.
Albarnaz, J.D., Ren, H., Torres, A.A., Shmeleva, E.V., Melo, C.A., Bannister, A.J., Brember, M.P., Chung, B.Y., Smith, G.L., 2022. Molecular mimicry of NF-κB by vaccinia virus protein enables selective inhibition of antiviral responses. Nat. Microbiol. 7, 154–168.
Alonso, R.C., Moura, P.P., Caldeira, D.F., Mendes, M.H., Pinto, M.H., Cargnelutti, J.F., Flores, E.F., de Sant'Ana, F.J., 2020. Poxviruses diagnosed in cattle from Distrito Federal, Brazil (2015–2018). Transbound. Emerg. Dis. 67, 1563–1573.
Anisimova, M., Bielawski, J.P., Yang, Z., 2002. Accuracy and power of bayes prediction of amino acid sites under positive selection. Mol. Biol. Evol. 19, 950–958.
Archard, L.C., Mackett, M., 1979. Restriction endonuclease analysis of red cowpox virus and its white pock variant. J. Gen. Virol. 45, 51–63.
Basile, W., Salvatore, M., Bassot, C., Elofsson, A., 2019. Why do eukaryotic proteins contain more intrinsically disordered regions? PLoS Comput. Biol. 15, e1007186.
Bay, R.A., Bielawski, J.P., 2011. Recombination detection under evolutionary scenarios relevant to functional divergence. J. Mol. Evol. 73, 273–286.
Beer, E.M., Rao, V.B., 2019. A systematic review of the epidemiology of human monkeypox outbreaks and implications for outbreak strategy. PLoS Negl. Trop. Dis. 13, e0007791.
Brandt, T., Heck, M.C., Vijaysri, S., Jentarra, G.M., Cameron, J.M., Jacobs, B.L., 2005. The N-terminal domain of the vaccinia virus E3L-protein is required for neurovirulence, but not induction of a protective immune response. Virology 333, 263–270.
Bratke, K.A., McLysaght, A., Rothenburg, S., 2013. A survey of host range genes in poxvirus genomes. Infect. Genet. Evol. 14, 406–425.
Brennan, G., Kitzman, J.O., Shendure, J., Geballe, A.P., 2015. Experimental evolution identifies vaccinia virus mutations in A24R and A35R that antagonize the protein kinase R pathway and accompany collapse of an extragenic gene amplification. J. Virol. 89, 9986–9997.
Brown, C.J., Johnson, A.K., Daughdrill, G.W., 2010. Comparing models of evolution for ordered and disordered proteins. Mol. Biol. Evol. 27, 609–621.
Broyles, S.S., 2003. Vaccinia virus transcription. J. Gen. Virol. 84, 2293–2303.
Bunge, E.M., Hoet, B., Chen, L., Lienert, F., Weidenthaler, H., Baer, L.R., Steffen, R., 2022. The changing epidemiology of human monkeypox-A potential threat? A systematic review. PLoS Negl. Trop. Dis. 16, e0010141.
Burles, K., Irwin, C.R., Burton, R.L., Schriewer, J., Evans, D.H., Buller, R.M., Barry, M., 2014. Initial characterization of vaccinia virus B4 suggests a role in virus spread. Virology 456-457, 108–120.
Cagliani, R., Forni, D., Filippi, G., Mozzi, A., De Gioia, L., Pontremoli, C., Pozzoli, U., Bresolin, N., Clerici, M., Sironi, M., 2016. The mammalian complement system as an epitome of host-pathogen genetic conflicts. Mol. Ecol. 25, 1324–1339.
Cardeti, G., Gruber, C.E.M., Eleni, C., Carletti, F., Castilletti, C., Manna, G., Rosone, F., Giombini, E., Selleri, M., Lapa, D., Puro, V., Di Caro, A., Lorenzetti, R., Scicluna, M. T., Grifoni, G., Rizzoli, A., Tagliapietra, V., De Marco, L., Capobianchi, M.R., Autorino, G.L., 2017. Fatal outbreak in tonkean macaques caused by possibly novel orthopoxvirus, Italy, January 2015 (1). Emerg. Infect. Dis. 23, 1941–1949.
Carpentier, D.C.J., Van Loggerenberg, A., Dieckmann, N.M.G., Smith, G.L., 2017. Vaccinia virus egress mediated by virus protein A36 is reliant on the F12 protein. J. Gen. Virol. 98, 1500–1514.
Carroll, D.S., Emerson, G.L., Li, Y., Sammons, S., Olson, V., Frace, M., Nakazawa, Y., Czerny, C.P., Tryland, M., Kolodziejek, J., Nowotny, N., Olsen-Rasmussen, M., Khristova, M., Govil, D., Karem, K., Damon, I.K., Meyer, H., 2011. Chasing Jenner's vaccine: revisiting cowpox virus classification. PLoS One 6, e23086.
Chen, N., Li, G., Liszewski, M.K., Atkinson, J.P., Jahrling, P.B., Feng, Z., Schriewer, J., Buck, C., Wang, C., Lefkowitz, E.J., Esposito, J.J., Harms, T., Damon, I.K., Roper, R. L., Upton, C., Buller, R.M., 2005. Virulence differences between monkeypox virus isolates from West Africa and the Congo basin. Virology 340, 46–63.
Cone, K.R., Kronenberg, Z.N., Yandell, M., Elde, N.C., 2017. Emergence of a viral RNA polymerase variant during gene copy number amplification promotes rapid evolution of vaccinia virus. J. Virol. 91, e01428, 16.
Cresawn, S.G., Prins, C., Latner, D.R., Condit, R.C., 2007. Mapping and phenotypic analysis of spontaneous isatin-beta-thiosemicarbazone resistant mutants of vaccinia virus. Virology 363, 319–332.
da Fonseca, F.G., Wolffe, E.J., Weisberg, A., Moss, B., 2000. Effects of deletion or stringent repression of the H3L envelope gene on vaccinia virus replication. J. Virol. 74, 7518–7528.
Darling, A.C., Mau, B., Blattner, F.R., Perna, N.T., 2004. Mauve: multiple alignment of conserved genomic sequence with rearrangements. Genome Res. 14, 1394–1403.

Darling, A.E., Mau, B., Perna, N.T., 2010. progressiveMauve: multiple genome alignment with gene gain, loss and rearrangement. PLoS One 5, e11147.
Davies, D.H., McCausland, M.M., Valdez, C., Huynh, D., Hernandez, J.E., Mu, Y., Hirst, S., Villarreal, L., Felgner, P.L., Crotty, S., 2005. Vaccinia virus H3L envelope protein is a major target of neutralizing antibodies in humans and elicits protection against lethal challenge in mice. J. Virol. 79, 11724–11733.
Doceul, V., Hollinshead, M., van der Linden, L., Smith, G.L., 2010. Repulsion of superinfecting virions: a mechanism for rapid virus spread. Science 327, 873–876.
Dosztanyi, Z., 2018. Prediction of protein disorder based on IUPred. Protein Sci. 27, 331–340.
Duggan, A.T., Klunk, J., Porter, A.F., Dhody, A.N., Hicks, R., Smith, G.L., Humphreys, M., McCollum, A.M., Davidson, W.B., Wilkins, K., Li, Y., Burke, A., Polasky, H., Flanders, L., Poinar, D., Raphenya, A.R., Lau, T.T.Y., Alcock, B., McArthur, A.G., Golding, G.B., Holmes, E.C., Poinar, H.N., 2020. The origins and genomic diversity of American Civil War Era smallpox vaccine strains. Genome Biol. 21, 175 .
Dyson, H.J., Wright, P.E., 2005. Intrinsically unstructured proteins and their functions. Nat. Rev. Mol. Cell Biol. 6, 197–208.
Elde, N.C., Child, S.J., Eickbush, M.T., Kitzman, J.O., Rogers, K.S., Shendure, J., Geballe, A.P., Malik, H.S., 2012. Poxviruses deploy genomic accordions to adapt rapidly against host antiviral defenses. Cell 150, 831–841.
Esteban, D.J., Hutchinson, A.P., 2011. Genes in the terminal regions of orthopoxvirus genomes experience adaptive molecular evolution. BMC Genom. 12, 261, 2164-12-261.
Fenner, F., Henderson, D.A., Arita, I., Jezek, Z., Ladnyi, I.D., 1988. Smallpox and its eradication, 6. World Health Organization, Geneva, pp. 1–1421.
Franke, A., Pfaff, F., Jenckel, M., Hoffmann, B., Höper, D., Antwerpen, M., Meyer, H., Beer, M., Hoffmann, D., 2017. Classification of cowpox viruses into several distinct clades and identification of a novel lineage. Viruses 9, 142.
Gao, J., Gigante, C., Khmaladze, E., Liu, P., Tang, S., Wilkins, K., Zhao, K., Davidson, W., Nakazawa, Y., Maghlakelidze, G., Geleishvili, M., Kokhreidze, M., Carroll, D.S., Emerson, G., Li, Y., 2018. Genome sequences of Akhmeta virus, an early divergent old world orthopoxvirus. Viruses 10, 252.
Gardner, A., Úbeda, F., 2017. The meaning of intragenomic conflict. Nat. Ecol. Evol. 1, 1807–1815.
Gigante, C.M., Gao, J., Tang, S., McCollum, A.M., Wilkins, K., Reynolds, M.G., Davidson, W., McLaughlin, J., Olson, V.A., Li, Y., 2019. Genome of Alaskapox virus, a novel orthopoxvirus isolated from Alaska. Viruses 11, 708.
Gilchuk, I., Gilchuk, P., Sapparapu, G., Lampley, R., Singh, V., Kose, N., Blum, D.L., Hughes, L.J., Satheshkumar, P.S., Townsend, M.B., Kondas, A.V., Reed, Z., Weiner, Z., Olson, V.A., Hammarlund, E., Raue, H.P., Slifka, M.K., Slaughter, J.C., Graham, B.S., Edwards, K.M., Eisenberg, R.J., Cohen, G.H., Joyce, S., Crowe, J.E., 2016. Cross-neutralizing and protective human antibody specificities to poxvirus infections. Cell 167, 684–694 e9.
Grimm, C., Hillen, H.S., Bedenk, K., Bartuli, J., Neyer, S., Zhang, Q., Hüttenhofer, A., Erlacher, M., Dienemann, C., Schlosser, A., Urlaub, H., Böttcher, B., Szalay, A.A., Cramer, P., Fischer, U., 2019. Structural basis of poxvirus transcription: vaccinia RNA polymerase complexes. Cell 179, 1537–1550 e19.
Guindon, S., Delsuc, F., Dufayard, J.F., Gascuel, O., 2009. Estimating maximum likelihood phylogenies with PhyML. Methods Mol. Biol. 537, 113–137.
Gyuranecz, M., Foster, J.T., Dán, Á., Ip, H.S., Egstad, K.F., Parker, P.G., Higashiguchi, J. M., Skinner, M.A., Höfle, U., Kreizinger, Z., Dorrestein, G.M., Solt, S., Sós, E., Kim, Y. J., Uhart, M., Pereda, A., González-Hein, G., Hidalgo, H., Blanco, J.M., Erdélyi, K., 2013. Worldwide phylogenetic relationship of avian poxviruses. J. Virol. 87, 4938–4951.
Hagai, T., Azia, A., Babu, M.M., Andino, R., 2014. Use of host-like peptide motifs in viral proteins is a prevalent strategy in host-virus interactions. Cell Rep. 7, 1729–1739.
Hatcher, E.L., Hendrickson, R.C., Lefkowitz, E.J., 2014. Identification of nucleotide-level changes impacting gene content and genome evolution in orthopoxviruses. J. Virol. 88, 13651–13668.
Hendrickson, R.C., Wang, C., Hatcher, E.L., Lefkowitz, E.J., 2010. Orthopoxvirus genome evolution: the role of gene loss. Viruses 2, 1933–1967.
Higley, S., Way, M., 1997. Characterization of the vaccinia virus F8L protein. J. Gen. Virol. 78 (Pt 10), 2633–2637.
Hudson, P.N., Self, J., Weiss, S., Braden, Z., Xiao, Y., Girgis, N.M., Emerson, G., Hughes, C., Sammons, S.A., Isaacs, S.N., Damon, I.K., Olson, V.A., 2012. Elucidating the role of the complement control protein in monkeypox pathogenicity. PLoS One 7, e35086.
Ishii, K., Moss, B., 2001. Role of vaccinia virus A20R protein in DNA replication: construction and characterization of temperature-sensitive mutants. J. Virol. 75, 1656–1663.
Jarahian, M., Fiedler, M., Cohnen, A., Djandji, D., Hämmerling, G.J., Gati, C., Cerwenka, A., Turner, P.C., Moyer, R.W., Watzl, C., Hengel, H., Momburg, F., 2011. Modulation of NKp30- and NKp46-mediated natural killer cell responses by poxviral hemagglutinin. PLoS Pathog. 7, e1002195.
Katoh, K., Standley, D.M., 2013. MAFFT multiple sequence alignment software version 7: improvements in performance and usability. Mol. Biol. Evol. 30, 772–780.
Kringelum, J.V., Lundegaard, C., Lund, O., Nielsen, M., 2012. Reliable B cell epitope predictions: impacts of method development and improved benchmarking. PLoS Comput. Biol. 8, e1002829.
Kryazhimskiy, S., Plotkin, J.B., 2008. The population genetics of dN/dS. PLoS Genet. 4, e1000304.
Kumar, N., Kaushik, R., Tennakoon, C., Uversky, V.N., Longhi, S., Zhang, K.Y., Bhatia, S., 2021. Comprehensive intrinsic disorder analysis of 6108 viral proteomes: from the extent of intrinsic disorder penetrance to functional annotation of disordered viral proteins. J. Proteome Res. 20, 2704–2713.
Leeks, A., West, S.A., Ghoul, M., 2021. The evolution of cheating in viruses. Nat. Commun. 12, 6928, 021-27293-6.
Lefkowitz, E., Wang, C., Upton, C., 2006. Poxviruses: past, present and future. Virus Res. 117, 105–118.
Lequime, S., Fontaine, A., Ar Gouilh, M., Moltini-Conclois, I., Lambrechts, L., 2016. Genetic drift, purifying selection and vector genotype shape dengue virus intra-host genetic diversity in mosquitoes. PLoS Genet. 12, e1006111.
Li, X., Giorgi, E.E., Marichannegowda, M.H., Foley, B., Xiao, C., Kong, X.P., Chen, Y., Gnanakaran, S., Korber, B., Gao, F., 2020. Emergence of SARS-CoV-2 through recombination and strong purifying selection. Sci. Adv. 6, eabb9153.
Lin, C.L., Chung, C.S., Heine, H.G., Chang, W., 2000. Vaccinia virus envelope H3L protein binds to cell surface heparan sulfate and is important for intracellular mature virion morphogenesis and virus infection *in vitro* and *in vivo*. J. Virol. 74, 3353–3365.
Lin, S., Chen, W., Broyles, S.S., 1992. The vaccinia virus B1R gene product is a serine/threonine protein kinase. J. Virol. 66, 2717–2723.
Liu, R., Mendez-Rios, J.D., Peng, C., Xiao, W., Weisberg, A.S., Wyatt, L.S., Moss, B., 2019. SPI-1 is a missing host-range factor required for replication of the attenuated modified vaccinia Ankara (MVA) vaccine vector in human cells. PLoS Pathog. 15, e1007710.
Liu, S.W., Katsafanas, G.C., Liu, R., Wyatt, L.S., Moss, B., 2015. Poxvirus decapping enzymes enhance virulence by preventing the accumulation of dsRNA and the induction of innate antiviral responses. Cell Host Microbe 17, 320–331.
Maluquer de Motes, C., Schiffner, T., Sumner, R.P., Smith, G.L., 2014. Vaccinia virus virulence factor N1 can be ubiquitylated on multiple lysine residues. J. Gen. Virol. 95, 2038–2049.
Martin, D., Rybicki, E., 2000. RDP: detection of recombination amongst aligned sequences. Bioinformatics 16, 562–563.
Martin, D.P., Murrell, B., Khoosal, A., Muhire, B., 2017. Detecting and analyzing genetic recombination using RDP4. Methods Mol. Biol. 1525, 433–460.
Martin, D.P., Varsani, A., Roumagnac, P., Botha, G., Maslamoney, S., Schwab, T., Kelz, Z., Kumar, V., Murrell, B., 2020. RDP5: a computer program for analyzing recombination in, and removing signals of recombination from, nucleotide sequence datasets. Virus Evol. 7, veaa087.
McFadden, G., 2005. Poxvirus tropism. Nat. Rev. Micro Biol. 3, 201–213.
McLysaght, A., Baldi, P.F., Gaut, B.S., 2003. Extensive gene gain associated with adaptive evolution of poxviruses. Proc. Natl. Acad. Sci. USA 100, 15655–15660.
Meng, X., Wu, X., Yan, B., Deng, J., Xiang, Y., 2013. Analysis of the role of vaccinia virus H7 in virion membrane biogenesis with an H7-deletion mutant. J. Virol. 87, 8247–8253.
Meszaros, B., Erdos, G., Dosztanyi, Z., 2018. IUPred2A: context-dependent prediction of protein disorder as a function of redox state and protein binding. Nucleic Acids Res. 46, W329–W337.
Meszaros, B., Simon, I., Dosztanyi, Z., 2009. Prediction of protein binding regions in disordered proteins. PLoS Comput. Biol. 5, e1000376.
Mirzakhanyan, Y., Gershon, P., 2019. The vaccinia virion: filling the gap between atomic and ultrastructure. PLoS Pathog. 15, e1007508.
Moss, B., 2013. Poxvirus DNA replication. Cold Spring Harb. Perspect. Biol. 5, a010199.
Mozzi, A., Biolatti, M., Cagliani, R., Forni, D., Dell'Oste, V., Pontremoli, C., Vantaggiato, C., Pozzoli, U., Clerici, M., Landolfo, S., Sironi, M., 2020a. Past and ongoing adaptation of human cytomegalovirus to its host. PLoS Pathog. 16, e1008476.
Mozzi, A., Forni, D., Cagliani, R., Clerici, M., Pozzoli, U., Sironi, M., 2020b. Intrinsically disordered regions are abundant in simplexvirus proteomes and display signatures of positive selection. Virus Evol. 6, veaa028.
Nichols, R.J., Wiebe, M.S., Traktman, P., 2006. The vaccinia-related kinases phosphorylate the N' terminus of BAF, regulating its interaction with DNA and its retention in the nucleus. Mol. Biol. Cell 17, 2451–2464.
Nilsson, J., Grahn, M., Wright, A.P., 2011. Proteome-wide evidence for enhanced positive Darwinian selection within intrinsically disordered regions in proteins. Genome Biol. 12, R65 .
Nuara, A.A., Walter, L.J., Logsdon, N.J., Yoon, S.I., Jones, B.C., Schriewer, J.M., Buller, R.M., Walter, M.R., 2008. Structure and mechanism of IFN-gamma antagonism by an orthopoxvirus IFN-gamma-binding protein. Proc. Natl. Acad. Sci. USA 105, 1861–1866.
Olson, A.T., Wang, Z., Rico, A.B., Wiebe, M.S., 2019. A poxvirus pseudokinase represses viral DNA replication via a pathway antagonized by its paralog kinase. PLoS Pathog. 15, e1007608.
Paradis, E., Schliep, K., 2019. ape 5.0: an environment for modern phylogenetics and evolutionary analyses in R. Bioinformatics 35, 526–528.
Peng, Z., Yan, J., Fan, X., Mizianty, M.J., Xue, B., Wang, K., Hu, G., Uversky, V.N., Kurgan, L., 2015. Exceptionally abundant exceptions: comprehensive characterization of intrinsic disorder in all domains of life. Cell Mol. Life Sci. 72, 137–151.
Posada, D., Crandall, K.A., 2001. Evaluation of methods for detecting recombination from DNA sequences: computer simulations. Proc. Natl. Acad. Sci. USA 98, 13757–13762.
Privman, E., Penn, O., Pupko, T., 2012. Improving the performance of positive selection inference by filtering unreliable alignment regions. Mol. Biol. Evol. 29, 1–5.
Pushker, R., Mooney, C., Davey, N.E., Jacque, J.M., Shields, D.C., 2013. Marked variability in the extent of protein disorder within and between viral families. PLoS One 8, e60724.
Resch, W., Weisberg, A.S., Moss, B., 2009. Expression of the highly conserved vaccinia virus E6 protein is required for virion morphogenesis. Virology 386, 478–485.
Santos, C.R., Blanco, S., Sevilla, A., Lazo, P.A., 2006. Vaccinia virus B1R kinase interacts with JIP1 and modulates c-Jun-dependent signaling. J. Virol. 80, 7667–7675.

Santos, C.R., Vega, F.M., Blanco, S., Barcia, R., Lazo, P.A., 2004. The vaccinia virus B1R kinase induces p53 downregulation by an Mdm2-dependent mechanism. Virology 328, 254–265.
Sanz, P., Moss, B., 1999. Identification of a transcription factor, encoded by two vaccinia virus early genes, that regulates the intermediate stage of viral gene expression. Proc. Natl. Acad. Sci. USA 96, 2692–2697.
Sarker, S., Isberg, S.R., Moran, J.L., Araujo, R.D., Elliott, N., Melville, L., Beddoe, T., Helbig, K.J., 2019. Crocodilepox virus evolutionary genomics supports observed poxvirus infection dynamics on saltwater crocodile (Crocodylus porosus). Viruses 11, 1116.
Sawyer, S., 1989. Statistical tests for detecting gene conversion. Mol. Biol. Evol. 6, 526–538.
Sela, I., Ashkenazy, H., Katoh, K., Pupko, T., 2015. GUIDANCE2: accurate detection of unreliable alignment regions accounting for the uncertainty of multiple parameters. Nucleic Acids Res. 43, W7–14.
Senkevich, T.G., Wyatt, L.S., Weisberg, A.S., Koonin, E.V., Moss, B., 2008. A conserved poxvirus NlpC/P60 superfamily protein contributes to vaccinia virus virulence in mice but not to replication in cell culture. Virology 374, 506–514.
Senkevich, T.G., Yutin, N., Wolf, Y.I., Koonin, E.V., Moss, B., 2021. Ancient gene capture and recent gene loss shape the evolution of orthopoxvirus-host interaction genes. mBio 12, e0149521, 21. Epub 2021 Jul 13.
Shannon, P., Markiel, A., Ozier, O., Baliga, N.S., Wang, J.T., Ramage, D., Amin, N., Schwikowski, B., Ideker, T., 2003. Cytoscape: a software environment for integrated models of biomolecular interaction networks. Genome Res. 13, 2498–2504.
Shchelkunov, S.N., Resenchuk, S.M., Totmenin, A.V., Blinov, V.M., Marennikova, S.S., Sandakhchiev, L.S., 1993. Comparison of the genetic maps of variola and vaccinia viruses. FEBS Lett. 327, 321–324.
Shisler, J.L., Isaacs, S.N., Moss, B., 1999. Vaccinia virus serpin-1 deletion mutant exhibits a host range defect characterized by low levels of intermediate and late mRNAs. Virology 262, 298–311.
Silva, N.I.O., de Oliveira, J.S., Kroon, E.G., Trindade, G.S., Drumond, B.P., 2020. Here, there, and everywhere: the wide host range and geographic distribution of zoonotic orthopoxviruses. Viruses 13, 43.
Simpson, K., Heymann, D., Brown, C.S., Edmunds, W.J., Elsgaard, J., Fine, P., Hochrein, H., Hoff, N.A., Green, A., Ihekweazu, C., Jones, T.C., Lule, S., Maclennan, J., McCollum, A., Mühlemann, B., Nightingale, E., Ogoina, D., Ogunleye, A., Petersen, B., Powell, J., Quantick, O., Rimoin, A.W., Ulaeato, D., Wapling, A., 2020. Human monkeypox - after 40 years, an unintended consequence of smallpox eradication. Vaccine 38, 5077–5081.
Sironi, M., Cagliani, R., Forni, D., Clerici, M., 2015. Evolutionary insights into host-pathogen interactions from mammalian sequence data. Nat. Rev. Genet. 16, 224–236.
Smith, J.M., 1992. Analyzing the mosaic structure of genes. J. Mol. Evol. 34, 126–129.
Smith, L.M., McWhorter, A.R., Shellam, G.R., Redwood, A.J., 2013. The genome of murine cytomegalovirus is shaped by purifying selection and extensive recombination. Virology 435, 258–268.
Smith, M.D., Wertheim, J.O., Weaver, S., Murrell, B., Scheffler, K., Kosakovsky Pond, S. L., 2015. Less is more: an adaptive branch-site random effects model for efficient detection of episodic diversifying selection. Mol. Biol. Evol. 32, 1342–1353.
Sood, C.L., Moss, B., 2010. Vaccinia virus A43R gene encodes an orthopoxvirus-specific late non-virion type-1 membrane protein that is dispensable for replication but enhances intradermal lesion formation. Virology 396, 160–168.
Sood, C.L., Ward, J.M., Moss, B., 2008. Vaccinia virus encodes I5, a small hydrophobic virion membrane protein that enhances replication and virulence in mice. J. Virol. 82, 10071–10078.
Szczerba, M., Subramanian, S., Trainor, K., McCaughan, M., Kibler, K.V., Jacobs, B.L., 2022. Small hero with Great powers: vaccinia virus E3 protein and evasion of the type I IFN response. Biomedicines 10, 235.
Trifinopoulos, J., Nguyen, L.T., von Haeseler, A., Minh, B.Q., 2016. W-IQ-TREE: a fast online phylogenetic tool for maximum likelihood analysis. Nucleic Acids Res. 44, W232–W235.
Tulman, E.R., Delhon, G., Afonso, C.L., Lu, Z., Zsak, L., Sandybaev, N.T., Kerembekova, U.Z., Zaitsev, V.L., Kutish, G.F., Rock, D.L., 2006. Genome of horsepox virus. J. Virol. 80, 9244–9258.
Turner, P.C., Moyer, R.W., 2008. The vaccinia virus fusion inhibitor proteins SPI-3 (K2) and HA (A56) expressed by infected cells reduce the entry of superinfecting virus. Virology 380, 226–233.
Upton, C., Slack, S., Hunter, A.L., Ehlers, A., Roper, R.L., 2003. Poxvirus orthologous clusters: toward defining the minimum essential poxvirus genome. J. Virol. 77, 7590–7600.
Walsh, I., Martin, A.J., Di Domenico, T., Tosatto, S.C., 2012. ESpritz: accurate and fast prediction of protein disorder. Bioinformatics 28, 503–509.
Wertheim, J.O., Kosakovsky Pond, S.L., 2011. Purifying selection can obscure the ancient age of viral lineages. Mol. Biol. Evol. 28, 3355–3365.
Xue, B., Blocquel, D., Habchi, J., Uversky, A.V., Kurgan, L., Uversky, V.N., Longhi, S., 2014. Structural disorder in viral proteins. Chem. Rev. 114, 6880–6911.
Yang, Z., 2007. PAML 4: phylogenetic analysis by maximum likelihood. Mol. Biol. Evol. 24, 1586–1591.
Zhang, L., Villa, N.Y., Rahman, M.M., Smallwood, S., Shattuck, D., Neff, C., Dufford, M., Lanchbury, J.S., Labaer, J., McFadden, G., 2009. Analysis of vaccinia virus-host protein-protein interactions: validations of yeast two-hybrid screenings. J. Proteome Res. 8, 4311–4318.
Zhang, W.H., Wilcock, D., Smith, G.L., 2000. Vaccinia virus F12L protein is required for actin tail formation, normal plaque size, and virulence. J. Virol. 74, 11654–11662.